Analysis of Biodiesel/Petroleum Diesel Blends with Comprehensive Two-Dimensional Gas Chromatography

John V. Seeley[1,*], Stacy K. Seeley[2], Elise K. Libby[1], and **James D. McCurry[3]**

[1]Oakland University, Department of Chemistry, Rochester, MI 48309; [2]Kettering University, Department of Science and Mathematics, Flint, MI 48504; and [3]Agilent Technologies, Inc., 2850 Centerville Road, Wilmington, DE 19808

Abstract

Comprehensive two-dimensional gas chromatography (GC×GC) is used to analyze petroleum diesel, biodiesel, and biodiesel/petroleum diesel blends. The GC×GC instrument is assembled from a conventional gas chromatograph fitted with a simple, in-line fluidic modulator. A 5% phenyl polydimethylsiloxane primary column is coupled to a polyethylene glycol secondary column. This column combination generates chromatograms where the fatty acid methyl esters (FAMEs) found in biodiesel occupy a region that is also populated by numerous cyclic alkanes and monoaromatics found in petroleum. Fortunately, the intensities of the petroleum hydrocarbon peaks are far lower than the intensities of the FAME peaks, even for blends with low biodiesel content. This allows the FAMEs to be accurately quantitated by direct integration. The method is calibrated by analyzing standard mixtures of soybean biodiesel in petroleum diesel with concentrations ranging from 1 to 20% v/v. The resulting calibration curve displays excellent linearity. This curve is used to determine the concentration of a B20 biodiesel/petroleum diesel blend obtained from a local retailer. Excellent precision and accuracy are obtained.

Introduction

The need for cleaner burning renewable motor fuels, combined with the high cost of crude oil, has sparked great interest in biodiesel production and distribution. Biodiesel is produced by the trans-esterification of vegetable oil or animal fats to produce fatty acid methyl esters (FAMEs). Worldwide, biodiesel is commonly sourced from soybean oil, rapeseed oil, and palm oil (1). The distribution of the individual FAMEs in pure biodiesel (B100) depends on the feedstock source. The relative amounts of each FAME can vary widely and have an effect on both fuel and handling properties (2). Pure biodiesel can be used directly or combined with petroleum-derived diesel. A number of industry standard methods have been developed by the European Committee for Standardization and ASTM International to ensure the quality of B100 as a blending stock. Many of these methods use single column gas chromatography (GC) to measure the major components and many key organic impurities in B100 (3–8). As a motor fuel, biodiesel is commonly blended with petroleum diesel at concentrations ranging from 1 vol% (B1) to 20 vol% (B20). The FAME content in biodiesel blends can be measured using GC; however, only one standard method has been published (9). The scope of this method only extends to biodiesel blends containing 5 vol% or lower FAME content. This method also requires a complex and costly sample preparation that uses liquid column chromatography to physically separate the FAMEs from the petroleum hydrocarbons before using GC to analyze the FAMEs. A variety of spectroscopic (10,11) and liquid chromatography (12,13) methods have also been tested for determining the levels of biodiesel in blended fuels.

Comprehensive two-dimensional gas chromatography (GC×GC) has been shown to be an effective approach for the characterization of petroleum-based fuels such as gasoline and diesel (14–29). Both flow modulation (23–25,27–29) and thermal modulation (14–22,26) have been employed. Thermal modulation strategies provide optimal resolution but often require the use of large amounts of liquid cryogen. In contrast, flow modulation yields lower resolution along the secondary dimension, but requires no additional consumables and uses simple, robust hardware (23,28,29).

Thermal modulation GC×GC has been applied to the analysis of FAMES in a variety of sample types (30–38). The majority of these studies have focused on characterizing the distribution of fats in food samples. DeMello et al. (39) recently used single-column GC and thermal modulation GC×GC to study the environmental processing of biodiesel and biodiesel blends. Their work demonstrated that FAMEs could be monitored with GC×GC in the presence of petroleum hydrocarbons; however, they did not test the quantitative accuracy and precision of using GC×GC to determine the composition of biodiesel blends.

This article presents a differential flow modulation GC×GC analysis of the FAME content in commercially blended biodiesel/petroleum diesel mixtures. A simple, in-line, fluidic modulator is employed. This modulator has been previously

* Author to whom correspondence should be addressed email: seeley@oakland.edu.

shown to be highly effective at analyzing the aromatic content of gasoline (28) and separating complex mixtures of volatile organic compounds (40).

Experimental

GC×GC apparatus

A schematic of the GC×GC system is shown in Figure 1. This system is similar to a previously described apparatus (28). An Agilent Technologies, Inc. (Wilmington, DE) 6890N GC was equipped with an Agilent 7683 Series Injector, electronic pneumatics, and dual flame-ionization detectors (FIDs). Samples were injected into a split inlet (1:250 split ratio, 250°C) that had an Agilent single taper, glass wool, deactivated liner (part number 51834711). Injected components were passed through an HP-5 primary column, modulated, and then further separated by passage through two parallel secondary columns. The run conditions are shown in Table I. All of the columns used were produced by Agilent Technologies, Inc.

The conversion of an Agilent 6890 GC into a GC×GC system required the addition of the three custom-built components: the modulator, electronics for controlling the modulator, and software for viewing the GC×GC chromatograms. A schematic of the modulator is shown in Figure 2. This device was constructed with deactivated fused silica tubing, two tee-unions (stainless steel, 100 µm i.d. orifices, VICI, Houston, TX, part number MT.5XCS6), and a three-port solenoid valve (Parker-General Valve, Fairfield, NJ, part number 009-0284-900). A 20 mL/min auxiliary flow of carrier gas supplied by the gas chromatograph was connected to the common port of the three-port solenoid valve. The solenoid valve was outside the column oven, while the remaining modulator parts were mounted on a thin piece of stainless steel sheet metal and housed inside the GC oven. The output ports of the solenoid valve were connected to the tee-unions with two pieces of 250-µm i.d. fused silica capillary tubing. The normally-closed port of the valve was connected to the upper tee union with an 8 cm long piece of capillary tubing. The upper tee was also the point where the flow exiting the primary column (1 mL/min) entered the modulator. The normally-open port of the valve was connected to the lower tee union with a 38 cm long piece of capillary tubing. The two tee unions were joined by a 15 cm × 450 µm i.d. piece of fused silica capillary tubing that served as the sample loop. A 10 cm long piece of 250 µm i.d. capillary tubing was connected from the bottom tee to a splitter union. The splitter union was connected to two secondary columns that were fed into independent FIDs.

Modulation was effected by the regular cycling of the solenoid valve every 1.50 s. The modulator was held in the "fill" state for 1.40 s and then switched to the "flush" state for 0.10 s. A custom electronic circuit was developed to control the modulator. The circuit allowed the modulation sequence to be started by the 6890 GC and synchronized with the detector data acquisition.

Table I. Summary of Chromatographic Conditions

Sample Introduction	**Oven**
0.2 µL injection size	50°C, 2.5 min
Split/Splitless Inlet, 250°C	Ramp to 260°C at 9°C/min,
1:250 split ratio	hold 8.0 min
Primary Column	**Detectors**
22.0 m × 250 µm HP-5,	FID, 250°C
0.25 µm film thickness	200 Hz sampling
Secondary Columns	**Modulator**
5.0 m × 250 µm DB-Wax,	1.50 s Modulation Period
0.10 µm film thickness	1.40 s Fill Time
5.0 m × 250 µm DB-210,	0.10 s Flush Time
0.25 µm film thickness	
Carrier Gas	
UHP Hydrogen	
1 mL/min primary flow	
20 mL/min auxiliary flow	

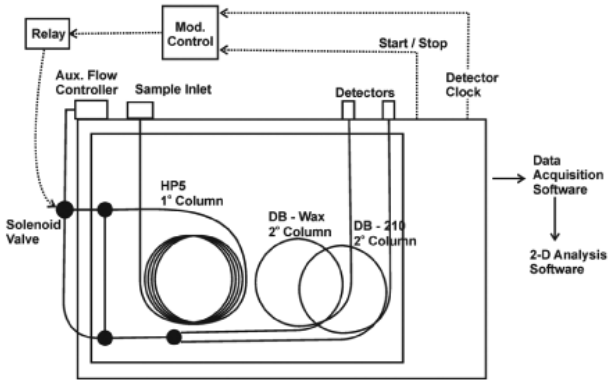

Figure 1. A schematic of the GC×GC apparatus. An Agilent 6890N gas chromatograph with dual flame ionization detectors was modified with modulator controller electronics, a solenoid valve, standard fittings, and custom software for analyzing the GC×GC chromatograms.

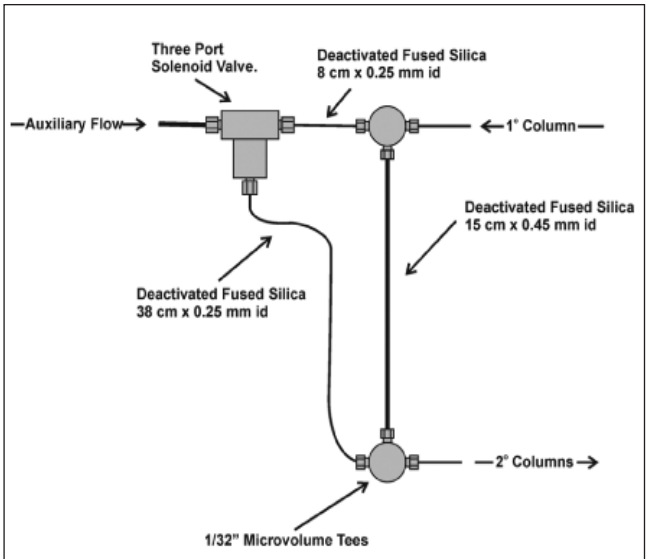

Figure 2. A schematic of the in-line fluidic modulator.

The performance of this modulator has been described, using gasoline as a test sample (28).

The detector signals were monitored with Agilent ChemStation software. The resulting 1-dimensional arrays were converted into 2-dimensional gas chromatograms using software developed in-house. For the purposes of this study, the 2-dimensional chromatograms generated by the DB-Wax secondary column produced the best separations of the petroleum diesel and the FAMEs. Thus, the chromatograms generated by the DB-210 secondary column were not used.

Quantitation was performed by first integrating the peaks in the original 1-dimensional FID signal array using Agilent ChemStation software. Custom software was then used to determine the primary and secondary retention times of each integrated peak and to assign each peak to a specific compound class (e.g., alkane, aromatic, C16 FAMEs, etc.).

Fuel samples

Eight pure biodiesel samples (B100) were obtained directly from several producers. The B100 samples were derived from soybean oil, rapeseed oil, palm oil, sunflower oil, peanut oil, poultry grease, pork grease, and coconut oil. Each B100 sample was dissolved in hexane (5% v/v) and analyzed by the GC×GC system to identify the major FAME compounds.

Quantitation of the FAME levels in biodiesel/petroleum diesel blends was performed using calibration curves generated from standard blends of soy biodiesel and #2 petroleum diesel. The #2 diesel sample was obtained from a retail commercial source. Calibration standards representing B1, B2, B5, B10, and B20 biodiesel blends (1%, 2%, 5%, 10%, and 20% v/v, respectively) were prepared by mixing B100 soy biodiesel with the #2 petroleum diesel. Calibration was done by summing the peaks areas for all of the C16 and C18 FAMEs peaks at each concentration level. Negligible amounts of C20 and C22 FAMEs were observed in the soy biodiesel. A sample of B20 biodiesel blend was obtained from a retail commercial vendor that used #2 diesel fuel and soybean B100 to prepare the blend. After calibration, two samples of this commercial B20 biodiesel blend were run five times each over three different days.

Results and Discussion

Modulator Operation

The principles of differential flow modulation have been described previously (41). A detailed analysis of the operation of the in-line fluidic modulator has also been presented (28). Briefly, the modulator operates by switching between two distinct states during each sampling cycle. The majority of the time, the device is in the "fill" state (see the left side of Figure 3). In this state, the primary flow enters the modulator at the upper tee union and the solenoid valve is set so that the auxiliary flow enters the modulator at the lower tee. The primary flow exits the upper tee union and heads toward the lower union through a conduit that serves as a sample loop. If left permanently in the "fill" state, the primary flow would pass through the sample loop until it eventually reached the lower union where it would combine with the auxiliary flow and exit out the third port toward the secondary column(s). However, modulation is effected by briefly placing the device in the "flush" state (see the right side of Figure 3) prior to the primary flow reaching the lower tee. The "flush" state is established by switching the solenoid valve so that the auxiliary flow is directed to the upper tee union. This high flow rate of the auxiliary carrier quickly sweeps the contents of the sample loop into the secondary column(s) as a pulse with a width that is much less than the modulation period. In addition, a brief pressure surge is generated at the upper tee union that temporarily halts the ingress of primary column effluent during the "flush" state. This greatly reduces the tailing of the outgoing concentration pulse. The magnitude of the pressure surge is controlled by the dimensions of the tubing connecting the solenoid valve to the modulator and the dimensions of the sample loop (28). The modulator is returned to the "fill" state after the collected primary effluent is swept from the sample loop. The continuous cycling between these two states creates a process where primary column peaks entering the device are converted into a series of sharp pulses, suitable for further separation in the secondary column(s).

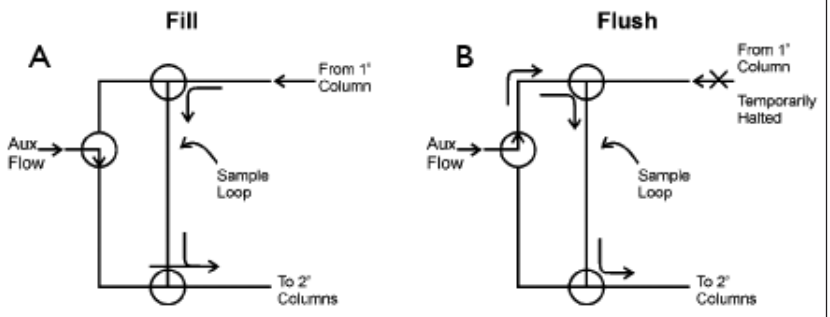

Figure 3. A schematic depicting the two states of the fluidic modulator. In the "fill" state (A), the auxiliary flow is directed to the bottom tee where it flows directly to the secondary columns. The primary column effluent enters the modulator at the top tee and flows through the sample loop. The modulator is briefly switched into the "flush" state (B) prior to the primary effluent reaching the bottom tee. In the "flush" state, the auxiliary flow is directed to the top tee and quickly sweeps the contents of the sample loop into the secondary columns and generates a pressure pulse that halts the inflow of primary flow. The modulator is returned to the "fill" state after the sample loop has been cleared of primary effluent.

The main advantage of differential flow modulation over thermal modulation is that large quantities of consumables (cryogenic fluid, cooling gas, etc.) are not required, nor are elaborate refrigeration units. Previous studies have shown (23,28) that differential flow modulation generates GC×GC chromatograms that are similar in structure to those produced by thermal modulation. However, differential flow modulation produces peaks with slightly larger widths along the secondary dimension. This is because differential flow modulation (unlike thermal modulation) does not spatially focus solutes eluting from the primary column. Instead, modulation is produced by combining the flow

emerging from the primary column with a much larger auxiliary flow. The combined fluid stream is then passed through the secondary column. The linear velocity in the secondary column is much higher than the value that produces optimal plate height. However, this negative aspect can be at least partially offset by using longer secondary columns and splitting the flow into two different secondary columns. Differential flow modulation also produces increased detector response over conventional single-column gas chromatography for detection schemes that respond to component flux (e.g., the FID). In principle, the signal increase should be similar to that observed for thermal modulation after an account is made for the portion of components split off downstream of the modulator (a 50% loss of components in this case) and the slightly increased peak widths.

GC×GC analysis of diesel

A typical chromatogram of petroleum-based diesel fuel is shown at the top of Figure 4. The structure of the chromatogram is very similar to those observed with thermal modulation, and with a previously described fluidic modulator (23). Peak widths at half maximum along the primary dimension are approximately 2.5 s. Saturated hydrocarbons have minimal secondary retention and a secondary width at half maximum of 55 ms. Mono-aromatic compounds display moderate secondary retention and have peak widths at half maximum of 65 ms, while di-aromatic compounds display the highest secondary retention and have peak widths at half maximum of 75 ms. These peak widths are in reasonable agreement with the value of 75 ms predicted for differential flow with a primary flow of 1 mL/min, secondary flow of 20 mL/min, and a modulation period of 1.5 s (23). Distinct "roof tile" bands of aromatic compounds having the same number of carbon atoms can be observed in the chromatogram. The three main compound classes (i.e., saturated hydrocarbons, mono-aromatics, and di-aromatics) occupy separate regions of the chromatogram for low to moderate primary retention; however, the saturated and mono-aromatic regions begin to converge at primary retention times greater than 850 s (i.e., at primary retention times after C_{13} alkanes elute).

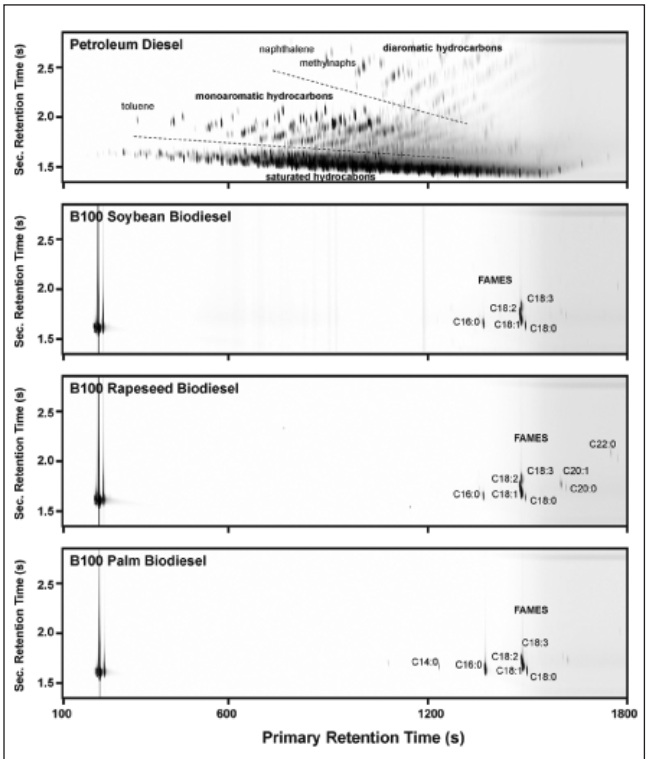

Figure 4. The GC×GC chromatograms of pure petroleum diesel and 3 types of pure biodiesel. The chromatograms are shown with high levels of signal amplification so that the minor constituents can be seen.

GC×GC analysis of pure biodiesel

Chromatograms of pure biodiesel (B100) produced from soybean oil, rapeseed oil, and palm oil are shown in the lower portion of Figure 4. The three B100 biodiesel samples have far fewer components than petroleum diesel. The identities of the individual FAMEs were confirmed through the analysis of FAME standards. Overall, the FAME peaks have strong primary column retention and moderate secondary column retention. The primary column elution is in order of increasing carbon number, with very little separation based on the level of unsaturation. This is clearly demonstrated by the four major C18 FAMEs: methyl stearate (C18:0), methyl oleate (C18:1), methyl linoleate (C18:2), and methyl linolenate (C18:3). These four compounds have primary retention times that fall within 13 s of one another. Along the secondary dimension (i.e., on the DB-Wax column), the FAMEs elute in order of increasing unsaturation. For instance, the secondary retention order of the C18 FAMEs is C18:0 < C18:1 < C18:2 < C18:3.

The observed distributions of FAMEs are different for each type of biodiesel. The soybean biodiesel sample was predominately composed of C18 FAMEs with a minor amount of methyl palmitate (C16:0). Rapeseed biodiesel had a C16 and C18 distribution similar to soybean biodiesel, but higher quantities of methyl eicosanoate (C20:0), methyl eicosenoate (C20:1), and methyl docosanoate (C22:0). Palm biodiesel had a similar FAME distribution to soybean biodiesel, but a lower amount of C18:3 and a higher amount of methyl myristate (C14:0).

Biodiesels derived from the less commonly used fats (sunflower oil, peanut oil, poultry grease, pork grease, and coconut oil) were also analyzed. The FAME distributions of these biodiesels were similar to the soybean, rapeseed, and palm biodiesels shown in Figure 4, with the exception of coconut oil biodeisel. Coconut biodiesel had much higher levels of short saturated FAMEs such as C8:0, C10:0, and C12:0.

These studies indicate that the current column combination is incapable of producing baseline resolution for several FAMEs that have the same carbon number but different levels of saturation (e.g., the C18:1 and C18:2 peaks are partially overlapped in each dimension). In a separate set of analyses, it was found that reversing the stationary phase order (i.e., DB-Wax primary column and an HP-5 secondary column) produced much better separations of the individual FAMEs. However, full resolution of the individual FAMEs is not required for accurate quantitation of the biodiesel levels in biodiesel blends. In fact, confining the FAMEs to a limited range of retention times decreases the likelihood of coelutions with the petroleum diesel components. Therefore, the HP-5 × DB-Wax column combination was employed for all quantitative studies.

GC×GC analysis of biodiesel blends

A chromatogram of a 5% v/v mixture of soybean biodiesel in #2 petroleum diesel is shown at the top of Figure 5. This figure shows that the C16 or larger FAMEs elute in a region of the two-dimensional chromatogram that also has components from petroleum diesel. Fortunately, the FAMEs do not elute along the intense *n*-alkane band located at the bottom of the chromatogram; instead, they elute in a region shared with cyclic alkanes and monoaromatics. This overlap is because the HP-5 × DB-Wax column combination exhibits a similar selectivity for FAMEs, cyclic alkanes, and monoaromatics. It is unlikely that operating under modulation conditions that produce narrower peaks along the secondary dimension would eliminate this problem. Fortunately, the petroleum cyclics and monoaromatics are at exceedingly small concentrations and highly overlapped with one another. This creates a rather homogenous increase in signal intensity due to petroleum hydrocarbons that is approximately 10 pA above the baseline. When FAMEs are present in the diesel fuel, the FAME peaks clearly stick out from this smooth region of the chromatogram. For example, the FAMEs in 5% biodiesel blends had average peak intensities that were greater than 400 pA above the baseline. Thus, the underlying, low intensity petroleum hydrocarbons could be considered as a locally elevated baseline and subtracted out during integration. This allows for the accurate quantitation of the FAME components in blends of the most commonly used sources of B100 (e.g., soybean oil, rapeseed oil, etc.).

It is important to note that biodiesel produced from tropical oils, such as coconut oil, have appreciable quantities of FAMEs with carbon numbers lower than C14 (1). Blends of such biodiesels with petroleum diesel would have FAME peaks that overlap with much more intense petroleum peaks. This makes the analyses of biodiesel blends prepared with B100 sourced from tropical oils more difficult than the blends examined in this work (i.e., a much more sophisticated subtraction strategy would have to be adopted to determine the proper areas of the FAME peaks).

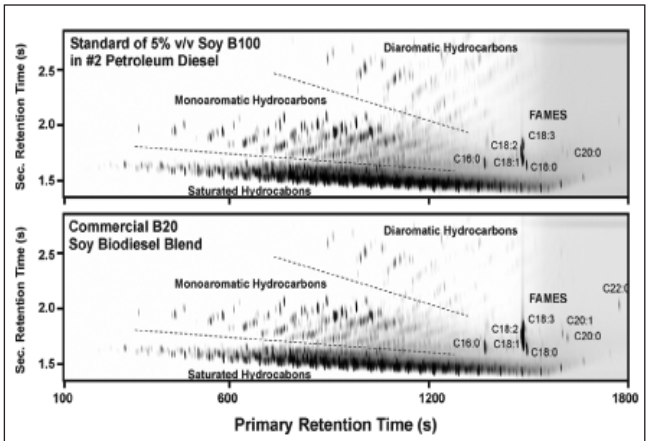

Figure 5. GC×GC analysis of a 5% v/v calibration standard and a B20 (20% v/v) commercial biodiesel blend.

Table II. Replicate Analysis of a B20 (20% v/v) Commercial Biodiesel Blend

Sample	Run Day	Fame Content (% v/v)
1	11 May 2006	19.4
2	11 May 2006	19.7
1	12 May 2006	19.9
2	12 May 2006	20.0
1	12 May 2006	20.2
2	12 May 2006	20.2
1	15 May 2006	19.8
2	15 May 2006	20.3
1	15 May 2006	20.4
2	15 May 2006	20.8
Average		20.1
Std Dev		0.4
RSD		1.9%

Quantitative analysis of biodiesel blends

A series of soybean biodiesel/petroleum diesel blends were prepared with biodiesel concentrations of 1, 2, 5, 10, and 20% v/v. The total peak areas due to the C16 and C18 FAMEs were plotted as a function of biodiesel concentration (see Figure 6). FAMEs other than C16 and C18 were negligible contributors to the total peak areas. The 5-point calibration curve had excellent linearity, with an R^2 value of 0.9999.

A commercial B20 biodiesel blend was obtained at a local retail station. The bottom portion of Figure 5 shows the chromatogram of the commercial sample. The FAME peaks were much larger than the other petroleum derived peaks. The calibration curve was used to determine the biodiesel concentration of the retail sample from the observed FAME areas. Replicate analyses (n = 10) of the commercial sample were made over a four-day period (Table II). The average calculated amount of biodiesel contained in this blend was determined to be 20.1% v/v with a standard deviation of 0.4% v/v. No independent analysis of this sample was available from the supplier; however, the results from the GC×GC analyses confirm that the sample was a 20% v/v biodiesel blend.

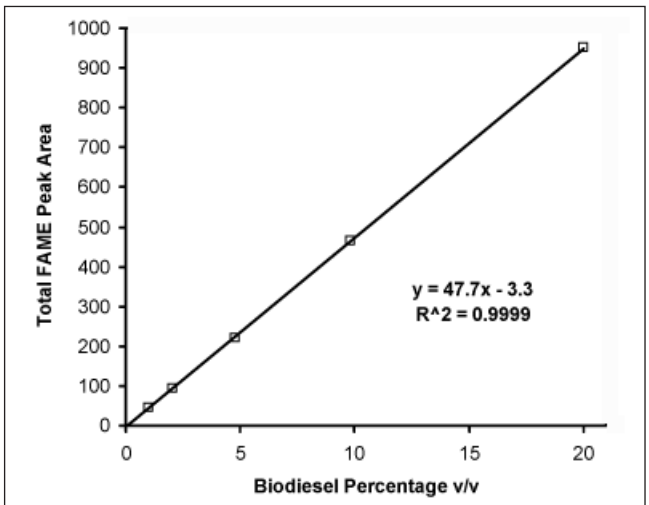

Figure 6. The calibration curve of the total peak area due to C16 and C18 FAMEs as a function of the percentage of soybean biodiesel in petroleum diesel.

The GC×GC instrument was used over a period of 3 months to perform numerous analyses of petroleum diesel, biodiesel, and blends. No decrease in chromatographic resolution along the primary or secondary dimensions was observed during this period. However, it should be noted that the trace quantities of diglycerides and triglycerides in biodiesel could eventually degrade the chromatographic resolution with extended use. Such contaminants would most likely be confined to the sample inlet or head of the primary column due to their low volatility.

Conclusions

A GC×GC instrument employing a simple, in-line fluidic modulator was used to analyze petroleum diesel fuel, a variety of biodiesels, and biodiesel/petroleum diesel blends. High-resolution separations were generated and the chromatograms of the blends displayed minimal overlap between the petroleum hydrocarbons and the biodiesel FAMEs. The biodiesel content of blended fuels was determined by directly integrating the FAME peaks and calculating the sum of the total area. A series of blends with biodiesel content ranging from 1% to 20% v/v were analyzed. A plot of total FAME area as a function of biodiesel content produced a calibration curve with excellent linearity and a very small *y*-intercept. A B20 (20 % v/v) commercial biodiesel blend was then quantitated and the results showed very good precision and excellent agreement with the manufacturer's stated biodiesel content. In addition to determining the biodiesel content, the GC×GC chromatograms can also be used to provide detailed information on the aromatic and non-aromatic hydrocarbons found in the fuel.

Acknowledgements

The authors would like to thank Agilent Technologies, Inc., for lending the 6890N gas chromatograph and supplying many of the consumables used for this study.

References

1. K.S. Tyson, J. Bozell, R. Wallace, E. Petersen, and L. Moens. "Biomass Oil Analysis: Research Needs and Recommendations, National Renewable Energy Laboratory," National Renewable Energy Laboratory, 2004.
2. K.S.a.M. Tyson, R.L. "2006 Biodiesel Handling Use and Guidelines, Third Ed.," National Renewable Energy Laboratory, 2006.
3. G. Knothe. Analyzing biodiesel: standards and other methods. *J. Am. Oil Chem. Soc.* **83:** 823–833 (2006).
4. EN14103 Fat and Oil Derivatives – Fatty Acid Methyl Esters (FAME) – Determination of Ester and Linolenic Acid Methyl Ester Contents; European Committee for Standardization: Management Centre, rue de Stassart 36, B-1050 Brussels., 2003.
5. EN14105 Fat and Oil Derivatives - Fatty Acid Methyl Esters (FAME) - Determination of Free and Total Glycerol and Mono-, Di- and Triglyceride Content; European Committee for Standardization: Management Centre, rue de Stassart 36, B-1050 Brussels, 2003.
6. EN14106 Fat and Oil Derivatives—Fatty Acid Methyl Esters (FAME)—Determination of Free Glycerol Content; European Committee for Standardization: Management Centre, rue de Stassart 36, B-1050 Brussels, 2003.
7. EN14110 Fat and Oil Derivatives – Fatty Acid Methyl Esters (FAME) – Determination of Methanol Content; European Committee for Standardization: Management Centre, rue de Stassart 36, B-1050 Brussels, 2003.
8. D6584 Test Method for Determination of Free and Total Glycerine in B-100 Biodiesel Methyl Esters by Gas Chromatography; ASTM International: 100 Barr Harbor Drive, West Conshohocken, PA, USA, 2003.
9. EN14331 Liquid Petroleum Products – Separation and Characterization of Fatty Acid Methyl Esters (FAME) From Middle Distillate Fuels; European Committee for Standardization: Management Centre, rue de Stassart 36, B-1050 Brussels, 2004.
10. G. Knothe. Determining the blend level of mixtures of biodiesel with conventional diesel fuel by fiber-optic near-infrared spectroscopy and H-1 nuclear magnetic resonance spectroscopy. *J. Am. Oil Chem. Soc.* **78:** 1025–1028 (2001).
11. M.F. Pimentel, G.M.G.S. Ribeiro, R.S. da Cruz, L. Stragevitch, J.G.A. Pacheco, and L.S.G. Teixeira. Determination of biodiesel content when blended with mineral diesel fuel using infrared spectroscopy and multivariate calibration. *Microchem. J.* **82:** 201–206 (2006).
12. T.A. Foglia, K.C. Jones, and J.G. Phillips. Determination of biodiesel and triacylglycerols in diesel fuel by LC. *Chromatographia* **62:** 115–119 (2005).
13. M. Kaminski, E. Gilgenast, A. Przyjazny, and G. Romanik. Procedure for and results of simultaneous determination of aromatic hydrocarbons and fatty acid methyl esters in diesel fuels by high performance liquid chromatography. *J. Chromatogr. A* **1122:** 153–160 (2006).
14. C.J. Venkatramani and J.B. Phillips. Comprehensive 2-dimensional gas-chromatography applied to the analysis of complex-mixtures. *J. Microcolumn Sep.* **5:** 511–516 (1993).
15. J. Blomberg, P.J. Schoenmakers, J. Beens, and R. Tijssen. Comprehensive two-dimensional gas chromatography (GC×GC) and its applicability to the characterization of complex (petrochemical) mixtures. *J. High Resolut. Chromatogr.* **20:** 539–544 (1997).
16. R.M. Kinghorn and P.J. Marriott. Comprehensive two-dimensional gas chromatography using a modulating cryogenic trap. *J. High Resolut. Chromatogr.* **21:** 620–622 (1998).
17. R.B. Gaines, G.S. Frysinger, M.S. Hendrick-Smith, and J.D. Stuart. Oil spill source identification by comprehensive two-dimensional gas chromatography. *Environ. Sci. Technol.* **33:** 2106–2112 (1999).
18. G.S. Frysinger and R.B. Gaines. Comprehensive two-dimensional gas chromatography with mass spectrometric detection (GC×GC–MS) applied to the analysis of petroleum. *J. High Resolut. Chromatogr.* **22:** 251–255 (1999).
19. J. Beens and U.A.T. Brinkman. The role of gas chromatography in compositional analyses in the petroleum industry. *Trends Anal. Chem.* **19:** 260–275 (2000).
20. C.M. Reddy, T.I. Eglinton, A. Hounshell, H.K. White, L. Xu, R.B. Gaines, and G.S. Frysinger. The West Falmouth oil spill after thirty years: the persistence of petroleum hydrocarbons in marsh sediments. *Environ. Sci. Technol.* **36:** 4754–4760 (2002).
21. F.C.Y. Wang, W.K. Robbins, F.P. Di Sanzo, and F.C. McElroy. Speciation of sulfur-containing compounds in diesel by comprehensive two-dimensional gas chromatography. *J. Chromatogr. Sci.* **41:** 519–523 (2003).
22. R.X. Hua, Y.Y. Li, W. Liu, J.C. Zheng, H.B. Wei, J.H. Wang, X. Lu, H.W. Kong, and G.W. Xu. Determination of sulfur-containing compounds in diesel oils by comprehensive two-dimensional gas chromatography with a sulfur chemiluminescence detector. *J. Chromatogr. A* **1019:** 101–109 (2003).
23. P.A. Bueno and J.V. Seeley. Flow-switching device for comprehensive two-dimensional gas chromatography. *J. Chromatogr. A* **1027:** 3–10 (2004).

24. K.J. Johnson, B.J. Prazen, D.C. Young, and R.E. Synovec. Quantification of naphthalenes in jet fuel with GC×GC–Tri-PLS and windowed rank minimization retention time alignment. *J. Sep. Sci.* **27:** 410–416 (2004).
25. J.W. Diehl and F.P. Di Sanzo. Determination of aromatic hydrocarbons in gasolines by flow modulated comprehensive two-dimensional gas chromatography. *J. Chromatogr. A* **1080:** 157–165 (2005).
26. C. Vendeuvre, R. Ruiz-Guerrero, F. Bertoncini, L. Duval, D. Thiebaut, and M.C. Hennion. Characterisation of middle-distillates by comprehensive two-dimensional gas chromatography (GC×GC): a powerful alternative for performing various standard analysis of middle-distillates. *J. Chromatogr. A* **1086:** 21–28 (2005).
27. N.J. Micyus, J.D. McCurry, and J.V. Seeley. Analysis of aromatic compounds in gasoline with flow-switching comprehensive two-dimensional gas chromatography. *J. Chromatogr. A* **1086:** 115–121 (2005).
28. J.V. Seeley, N.J. Micyus, J.D. McCurry, and S.K. Seeley. Comprehensive two-dimensional gas chromatography with a simple fluidic modulator. *Am. Lab. News* **38:** 24–26 (2006).
29. J.V. Seeley, N.J. Micyus, S.V. Bandurski, S.K. Seeley, and J.D. McCurry. Microfluidic Deans switch for comprehensive two-dimensional gas chromatography. *Anal. Chem.* **79:** 1840–1847 (2007).
30. H.J. de Geus, I. Aidos, J. de Boer, J.B. Luten, and U.A.T. Brinkman. Characterisation of fatty acids in biological oil samples using comprehensive multidimensional gas chromatography. *J. Chromatogr. A* **910:** 95–103 (2001).
31. R.J. Western, S.S.G. Lau, P.J. Marriott, and P.D. Nichols. Positional and geometric isomer separation of FAME by comprehensive 2-D GC. *Lipids* **37:** 715–724 (2002).
32. L. Mondello, P.Q. Tranchida, R. Costa, A. Casilli, P. Dugo, A. Cotroneo, and G. Dugo. Fast GC for the analysis of fats and oils. *J. Sep. Sci.* **26:** 1467–1473 (2003).
33. M. Adahchour, L.L.P. van Stee, J. Beens, R.J.J. Vreuls, M.A. Batenburg, and U.A.T. Brinkman. Comprehensive two-dimensional gas chromatography with time-of-flight mass spectrometric detection for the trace analysis of flavour compounds in food. *J. Chromatogr. A* **1019:** 157–172 (2003).
34. L. Mondello, A. Casilli, P.Q. Tranchida, R. Costa, B. Chiofalo, P. Dugo, and G. Dugo. Evaluation of fast gas chromatography and gas chromatography-mass spectrometry in the analysis of lipids. *J. Chromatogr. A* **1035:** 237–247 (2004).
35. E. Jover, M. Adahchour, J.M. Bayona, R.J.J. Vreuls, and U.A.T. Brinkman. Characterization of lipids in complex samples using comprehensive two-dimensional gas chromatography with time-of-flight mass spectrometry. *J. Chromatogr. A* **1086:** 2–11 (2005).
36. S. de Koning, H.G. Janssen, M. van Deursen, and U.A.T. Brinkman. Automated on-line comprehensive two-dimensional LC×GC and LC×GC–ToF MS: instrument design and application to edible oil and fat analysis. *J. Sep. Sci.* **27:** 397–409 (2004).
37. S. de Koning, H.G. Janssen, and U.A.T. Brinkman. Characterization of triacylglycerides from edible oils and fats using single and multi-dimensional techniques. *LC-GC Europe* **19:** 590 (2006).
38. P. Tranchida, P. Donato, P. Dugo, G. Dugo, and L. Mondello. Comprehensive chromatographic methods for the analysis of lipids. *Trends Anal. Chem.* **26:** 191–205 (2007).
39. J.A. DeMello, C.A. Carmichael, E.E. Peacock, R.K. Nelson, J.S. Arey, and C.M. Reddy. Biodegradation and environmental behavior of biodiesel mixtures in the sea: An initial study. *Mar. Pollut. Bull.* **54:** 894–904 (2007).
40. J.V. Seeley, S.K. Seeley, and N.J. Primeau. Development and Application of Comprehensive Two-Dimensional Gas Chromatography With Flow Switching Modulation. *Abs. Pap. Am. Chem. Soc.* **230:** U337–U338 (2005).
41. J.V. Seeley, F. Kramp, and C.J. Hicks. Comprehensive two-dimensional gas chromatography via differential flow modulation. *Anal. Chem.* **72:** 4346–4352 (2000).

Manuscript received April 30, 2007;
revision received July 31, 2007.